2008 International Symposium on Nonlinear Theory and its Applications
NOLTA'08, Budapest, Hungary, September 7-10, 2008

# Synchronization of Model Neurons to AM Auditory Stimuli

Stefan Martignoli† and Ruedi Stoop†

†Institute of Neuroinformatics, UZH / ETH Zurich, Switzerland
Email: mstefan@ini.phys.ethz.ch, ruedi@ini.phys.ethz.ch

**Abstract**—Auditory nerve fibers transmit very precise timing information about incoming soundwaves from the inner hair cells (IHC) of the cochlea to the auditory nuclei of the brain. In this study, we investigate the response of a three-component model cochlea-IHC-auditory nerve. We show that the temporal and spectral characteristics of auditory nerve responses to amplitude-modulated (AM) tones reproduce biophysical measurements, and are a consequence of the synchronization of neurons upon the driving signal. To show the robustness and generality of this phenomenon, we investigate the Arnold tongues corresponding to a neuron model with stable limit-cycle dynamics driven by a sinusoidal. Finally, we discuss the contribution of the cochlear nonlinearities on the form of the resulting spiking patterns.

## 1. Introduction

The dynamics of regularly spiking neurons are described in a mathematical sense by stable limit-cycle oscillations [1]. The coupling of limit-cycle oscillators is in many ways well understood, see e.g. [2]. It is described by phase- and frequency-locking (a generalized synchronization scheme) along Arnold tongues. For coupled neurons driven by constant currents, a computational model has been developed [1], where a phase-locked computation relates the linear relationship between input current and intrinsic spiking frequencies to the resulting periodic spiking pattern of the corresponding Arnold tongue. A situation where this model could be of importance is the auditory peripheral neural system. Cochlea oscillations, locally amplified by the outer hair cells (OHC) are transferred by the inner hair cells (IHC) to the auditory nerve fibers by its mainly voltage-dependent ion-channels in the form of oscillations on top of a constant DC-current (see, e.g. [3]). It is known that the auditory nerve passes very precise information about the cochlea oscillation to the auditory nuclei [3], where phase-locked computation is a candidate to compute the pitch of a complex sound [4]. To this end, we are interested to test whether generic synchronization schemes [2] are able to explain physiological measurements [5, 6] from auditory nerve fibers. We choose a novel discrete neuron model [7, 8] because of its simplicity, preserving the limit-cycle property. We simulate the cochlea oscillations by a nonlinear electronic Hopf-cochlea [9, 10], followed by a model of IHC [11]. In section 2, the three models are introduced. The general synchronization scheme for sinusoidally driven regularly spiking neurons is verified in section 3. In section 4, the three models are connected, and the synchronization profile for pure tone stimulation is derived. Amplitude-modulated (AM) auditory stimuli are used in section 5 to test whether synchronization of the model neuron upon the driving waveform is able to account for experimental results. Finally, we discuss the importance of cochlear processing in shaping the information transmitted to the auditory nuclei.

## 2. Model elements description

**Hopf cochlea:** Recently, we have developed a biomorphic electronic Hopf-cochlea [9, 10]. The core of this electronic hearing sensor is a cascade of subcritical Hopf oscillators with characteristic frequencies $cf$, modeling the local amplification by the OHC. Each amplifier is followed by a 6th-order Butterworth filter modeling the viscous fluid. In this way, we have created a very robust and sensitive hearing sensor. It has been shown that the sensor successfully reproduces the characteristics of mam-

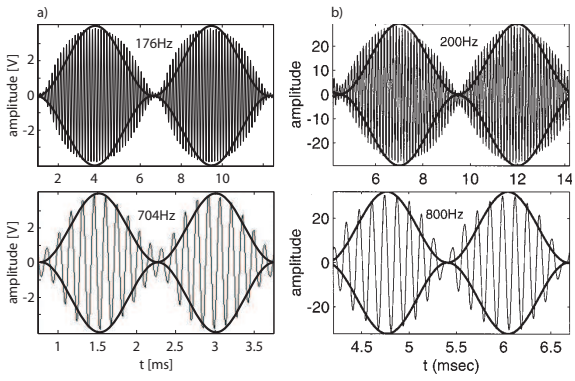


Figure 1: Envelope distortions of 100% amplitude-modulated input tones (bold lines: ideal sinusoidal envelopes). a) electronic Hopf-cochlea: Measurement: $cf = f_{carrier} = 7.04$kHz, $f_{mod} = 176$Hz (upper) and $f_{mod} = 704$Hz (lower figure), respectively (adapted from [10]). b) Chinchilla cochlea, $cf = f_{carrier} = 8$kHz, $f_{mod} = 200$Hz (upper) and $f_{mod} = 800$Hz (lower figure), respectively (adapted from [12]).

malian hearing, that is: the compressive nonlinearity, the high sensitivity for weak sounds and the nonlinear phenomena of two-tone suppression and combination tone generation [9, 10].
For AM signals, the stimuli used in this contribution, our Hopf cochlea responds almost undistinguishable to biological measurements, see the asymmetric distortion of the envelope in Fig. 1.

**Inner hair cells:** The inner hair cells (IHC) are implemented in software due to the currently most detailed model [11]. It implements the differential equation for the membrane voltage $V(t)$,

$$\dot{V} = \frac{1}{C_1}((V_1-V)g_T(U)+(V_2-V)g_f(V)+(V_3-V)g_s(V)), \tag{1}$$

where the transfer function $g_T(U)$ relates the cilia displacement $U$ to an internal conductance of the model. It has the form of a second-order Boltzmann function [11]. $g_f$ and $g_s$, the models internal sigmoid nonlinearities, represent fast respectively slow Potassium currents, see [11] for details and parameter values.

**Rulkov model neurons:** The neuron model used in this contribution has been introduced by N.F. Rulkov in 2002 [7]. It is a phenomenological model based on the limit-cycle property of biological neurons, implemented as a two-dimensional discrete map. It is given by the mapping

$$x_{n+1} = f_\alpha(x_n, x_{n-1}, y_n + \beta_n), \tag{2}$$
$$y_{n+1} = y_n - \mu(x_n + 1) + \mu\sigma + \mu\sigma_n, \tag{3}$$

where $x_n$ is the fast and $y_n$ is the slow dynamical variable. Parameters $\alpha$ and $\sigma$ are control parameters that select the desired spiking behavior. Input variables $\beta_n = \beta_e \cdot I_n$ and $\sigma_n = \sigma_e \cdot I_n$ are proportional to the synaptic input current $I_n$. The nonlinear function $f_\alpha$ is given by:

$$f_\alpha(x_n, x_{n-1}, u) = \begin{cases} \frac{\alpha}{1-x_n} + u & x_n \le 0 \\ \alpha + u & 0 < x_n < \alpha + u \quad \text{and} \quad x_{n-1} \le 0 \\ -1 & x_n \ge \alpha + u \quad \text{or} \quad x_{n-1} > 0 \end{cases} \tag{4}$$

If $\alpha < 4$, there is no bursting in the model. In the absence of synaptic inputs for $\alpha < 4$, the model converges to a stable fixed point for $\sigma < \sigma_{th} = 2 - \sqrt{\alpha/(1-\mu)}$ and shows regular spiking behavior (a limit-cycle) for $\sigma > \sigma_{th}$ with an almost linear dependence of the spiking frequency $f_{spikes}$ on the DC input current $I_{DC}$, see [8]. In this contribution, we use the parameter values for the regular spiking (RS) neuron $\alpha = 3.65, \sigma = 0.06, \mu = 0.0005, \sigma_e = 1, \beta_e = 0.133$, respectively a slightly modified version of Eqs. 2 and 4 that accounts for spike-afterhyperpolarization and models a fast spiking (FS) neuron, see [8].

## 3. Simplified model: Sinusoidally driven regularly spiking neurons

In the situation, where a limit-cycle neuron is driven by a waveform with both an DC and AC component, the DC component determines the intrinsic spiking frequency $f_0$ of the neuron. The additional AC component acts as a driving frequency $f_{drive}$. For weak interaction strength, depending on the value of the frequency ratio $f_0/f_{drive}$, phase-locking along Arnold tongues can be expected, see e.g. [2]. In this section, we verify this property for Rulkov neurons and determine the size of the phase-locked regions. For the value of $I^{DC} = 0.1$ in the RS neuron, leading to a spiking frequency of $f_0 = 0.01129$ spikes/iteration= 225.8 Hz, the neuron is driven by a sinusoidal input current $I^{AC}(t) = A \sin 2\pi f_{drive} t$ (time conversion slightly modified if compared to [8], $\sim 90$ input samples between two spikes). For this setting, we evaluate the winding number $\omega$, defined as

$$\omega = \frac{\sharp\text{intrinsic oscillations}}{\sharp\text{oscillations of the forcing}}. \tag{5}$$

Depending on the ratio $\Omega = f_0/f_{drive}$, the neuron synchronizes in different regimes of the winding number $\omega$, see Fig. 2. The overall picture of synchronization along Arnold tongues is obtained in Fig. 3, where the winding number $\omega$ is plotted against $\Omega$ in Fig. 3a at $A = 0.05$, and as a function of both $\{\Omega, A\}$ in Fig. 3b. In both figures, plateaus of constant rational winding numbers $\omega = p/q$, $p, q \in \mathbb{N}$ indicate regions of stable phase- and frequency-locking. Observations:
- The characteristic staircase of Fig. 3a demonstrates

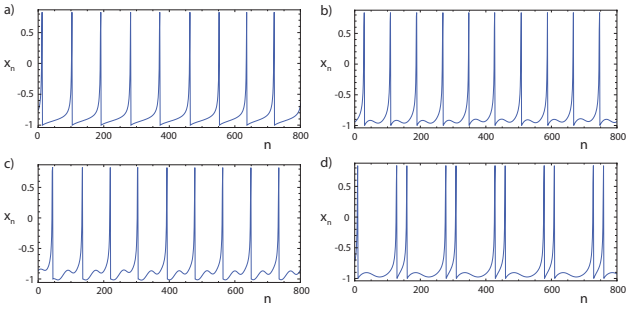


Figure 2: Synchronization in the sinusoidally driven Rulkov model. Spiketrain of the fast variable $x_n$ as a function of discrete timesteps $n$. The neuron receives an input current $I(t) = I^{DC} + I^{AC} = 0.1 + A \sin 2\pi f_{drive} t$. a) Unperturbed, A=0: The neuron is regularly spiking with intrinsic frequency $f_0 = 0.01129$ spikes / iteration. b) $A = 0.05$, $\Omega = f_0/f_{drive} = 0.9$, 1/1-locking. c) $A = 0.05$, $\Omega = 0.48$, 1/2-locking. d) $A = 0.05$, $\Omega = 1.7$, 2/1-locking.

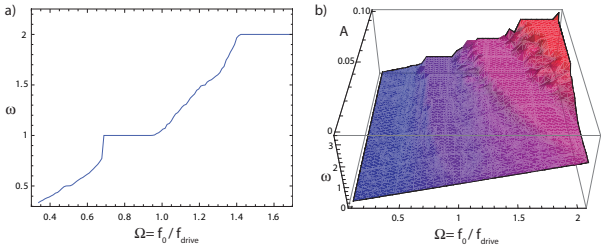


Figure 3: Arnold tongues in the sinusoidally driven Rulkov model. a) Winding number $\omega$ as a function of the frequency ratio $\Omega = f_0/f_{drive}$ at fixed interaction strength $A = 0.05$. Typical plateaus show the Arnold tongues of stable phase-locking. b) Threedimensional plot of $\omega$ as a function $\Omega, A$. Plateaus show the size of the Arnold tongues.

that Arnold tongues exist for all rational winding numbers $\omega = p/q$, although their widths rapidly decrease with increasing periodicity $q$.
- Moreover, the plateaus in Fig. 3 show that only the tongues with integer $\omega$ occupy a large portion of the parameter space $\{\Omega, A\}$.
- The Arnold tongues are shifted towards smaller values of $\Omega$; the sinusoidal driving thus has an excitatory effect on the neurons spiking behavior.

## 4. Full model: Response to pure tone stimulation

In this section, we connect the three models cochlea-IHC-neuron in a way that accounts for experimental results. Generally, a sampling rate of 20kHz is used and matched to a timestep of the fast spiking (FS) neuron model. The cochlea sections amplify input tones in a frequency- and amplitude-dependent way around their pre-defined $cf$, see [9]. It is relatively easy to match the cochlea output to a cilia displacement of the IHC by scaling the maximal voltage of 10V to a maximal displacement of 100nm [11].

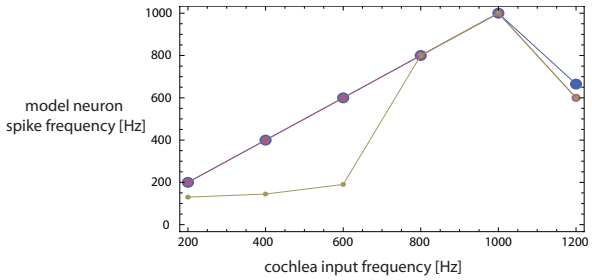


Figure 4: Input vs. output frequency characteristics at $cf = 800$ Hz. The colors label the cochlea input intensities: $-40dB(10V)$ (blue),$-50dB(10V)$ (purple),$-60dB(10V)$ (green). The model neuron synchronizes to the input up to $\sim 1kHz$ for strong inputs; at low intensities it looses synchronization outside the frequency band around $cf = 800$Hz.

Then, the IHC output is matched to the synaptic neuron input such that the intrinsic neuron oscillation resulting from the DC-component of the IHC output $V_{out}^{IHC}$ synchronizes to its AC-component for frequencies up to $\sim 1.2cf$, and cochlea input intensities down to at least $-50$dB(10V). The choice of a simple proportionality factor relating $I_n$ and $V_{out}^{IHC}$ is justified by the fact that synapses to auditory nerve fibers have mainly voltage-dependent ion channels [3]. The values that generate correct input vs. output frequency characteristics at $cf = 800$Hz in Fig. 4 are: $I_n = 40\cdot(V_{out}^{IHC} - V_{Rest}^{IHC}) + 0.02$, where $V_{Rest}^{IHC} = -0.058$ is the resting potential of the IHC.

## 5. Temporal and spectral characteristics of responses to AM stimuli

At this point, it is of interest whether the pure tone setting of the previous section is able to reproduce experimental results for complex sounds. We choose amplitude-modulated (AM) tones for several reasons: They are easy to be generated and exploit the nonlinear features of the Hopf-Cochlea (combination tones).

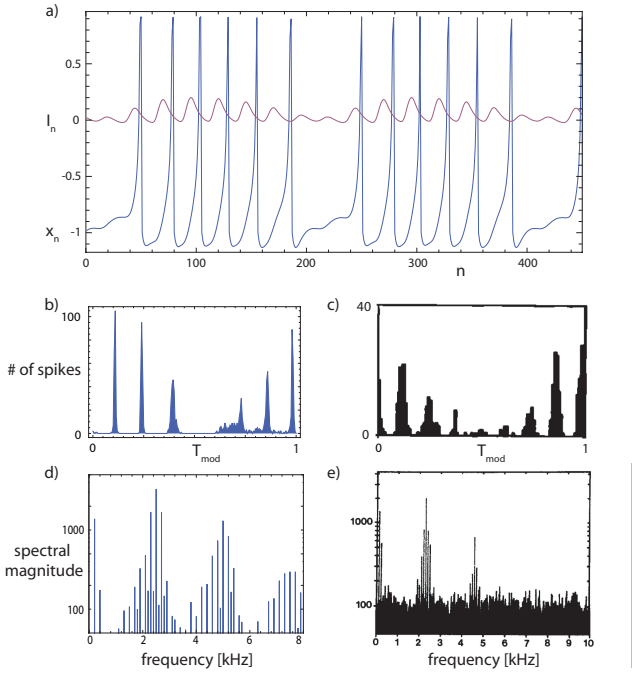


Figure 5: Model neuron response to AM stimuli. a) Model neuron spiketrain of the fast variable $x_n$ (blue) and synaptic input current $I_n$ (purple) as a function of timestep $n$. $cf = 800$Hz, $f_{carrier} = 800$Hz, $f_{mod} = 100$Hz. b,c): Comparison of temporal model response including gaussian noise at the synaptic input b) with experimental data c) (adapted from [5]). The spikes are counted with respect to the period of the modulation. $cf = 800$Hz, $f_{carrier} = 800$Hz, $f_{mod} = 100$Hz. d,e) Comparison of spectral model response d) with experimental data e) (adapted from [6]). $cf = 2.3$kHz, $f_{carrier} = 2.3$kHz, $f_{mod} = 100$Hz. For comments see text.

Experiments with AM sounds play a major role in the understanding of human pitch perception [4], and there are several physiological measurements of auditory nerve fibers available [5, 6].
For a stimulation of the cochlea at $cf = 800$Hz with $f_{carrier} = 800$Hz, $f_{mod} = 100$Hz in Fig. 5a, the neuron responds with a periodic spiking pattern (blue line in Fig. 5a). A close inspection reveals that the neuron synchronizes to those IHC oscillations (purple line in Fig. 5a) that are large enough to trigger spikes. Because of the slow variable $y_n$, there is a phase shift compared to the IHC output. In this noise-free simulation, there is no spike jitter, what makes it somewhat difficult to compare the model response to the biological data of Fig. 5c from [5]. Therefore, we add a gaussian random noise with mean 0 and variance $\kappa$ to the synaptic input $I_n$. The spontaneous neuron spiking rate then depends linearly on $\kappa$, not shown. We choose a spontaneous rate of $\sim 10$Hz at $\kappa = 0.075$, as measured in Fig. 5c. The AM stimulus is exposed to the cochlea for 60 seconds. Spikes are counted in a period histogram relative to the modulation period of the signal in Fig. 5b. To compare the model output with the spectral measurement Fig. 5e from [6] at $cf = 2.3$kHz, $f_{carrier} = 2.3$kHz, $f_{mod} = 100$Hz, the same procedure as above (pure tone stimulation, noise, period histogram) is repeated, and the period histogram is Fourier transformed to obtain the final spectrum of Fig. 5d. Although the spike jitter of Figs. 5b,d has been introduced artificially, the figures show a close match to the biological measurements. We therefore conclude that the forms of the period histogram Fig. 5c and auditory nerve spectrum Fig. 5e are a direct consequence of the neuron synchronization upon the stimulus as observed in Fig. 5a.

## 6. Discussion

In this contribution, we have verified for the Rulkov model that the synchronization of a limit-cycle neuron to a time-continuous waveform is a rather general phenomenon, and can be explained within the theory of locking along Arnold tongues. The Rulkov model neuron was then tested to serve as a model of auditory nerve fibers. The main problem was to realistically model the transmission from the IHC output to the synaptic input of the neuron. However, a simple scaling by a proportionality factor leads over a large interval to a persistent synchronization upon the auditory stimulus. Moreover, the resulting firing patterns remain stable throughout this interval, and are astonishingly close to biological measurements. We thus conclude that the synchronization ability of the neurons is enough to explain the form of the resulting firing patterns.
From our experiments, we are able to discuss the influence of the Hopf-cochlea nonlinearities onto the spike-trains in auditory nerve fibers. In the time domain, the asymmetric distortion of the envelope Fig. 1 leads to a broadening of the range in the envelope, where carrier frequency oscillations are able to trigger synchronized spikes in Fig. 5a, leading to the experimentally observed number of peaks in Fig. 5c. In the frequency domain, combination tone generation by the Hopf-cochlea is responsible for all peaks other than $\{f_{carrier}, f_{carrier} \pm f_{mod}\}$ (and multiples thereof introduced by the Fourier transform) in Fig. 5d. The cochlea thus represents the major processing stage of the signal before arriving at the auditory nuclei. According to our study, the role of auditory nerve fibers at low $cf$ is to synchronize upon the signal and thus to transmit the cochlea output characteristics.

## References


[1] R. Stoop, K. Schindler and L.A. Bunimovich, "Neocortical networks of pyramidal neurons: from local locking and chaos to macroscopic chaos and synchronization", *Nonlinearity*, vol.13, no. 5, 2000.

[2] G.V. Osipov, J. Kurths and C. Zhou, *Synchronization in Oscillatory Networks,* Springer, Berlin Heidelberg, 2007.

[3] C.D. Geisler, *From Sound to Synapse*, Oxford Univ. Press, Oxford, UK, 1998.

[4] J.H.E. Cartwright, D.L. González and O. Piro, "Nonlinear Dynamics of the Perceived Pitch of Complex Sounds", *Phys. Rev. Lett.*, vol.82, no.25, pp.5389–5392, 1999.

[5] E. Javel, "Coding of AM tones in the chinchilla auditory nerve: Implications for the pitch of complex tones," *J. Acoustic. Soc. Am.*, vol.68 (1), pp.133–146, 1980.

[6] S.M. Khanna and M.C. Teich, "Spectral characteristics of the responses of primary auditory-nerve fibers to amplitude-modulated signals," *Hearing Research*, vol.39, pp.143–158, 1989.

[7] N.F. Rulkov "Modeling of spiking-bursting neural behavior using two-dimensional map" *Phys. Rev. E,* vol.65, 041922, 2002

[8] N.F. Rulkov, I. Timofeev and M. Bazhenov, "Oscillations in Large-Scale Cortical Networks: Map-Based Model," *J. Comp. Neurosci.*, vol.17, pp.203-223, 2004.

[9] S. Martignoli, J.-J. van der Vyver, A. Kern, Y. Uwate, and R. Stoop, "Analog electronic cochlea with mammalian hearing characteristics", *Appl. Phys. Lett.* vol.91, 064108, 2007.

[10] R. Stoop, T. Jasa, Y. Uwate and S. Martignoli "From Hearing to Listening: Design and Properties of an Actively Tunable Electronic Hearing Sensor," *Sensors*, vol.7, pp.3287–3298, 2007.

[11] E.A. Lopez-Poveda and A. Eustaquio-Martin, "A Biophysical Model of the Inner Hair Cell: The Contribution of Potassium Currents to Peripheral Auditory Compression" *JARO* vol.7, pp.218-235, 2006.

[12] W.S. Rhode and A. Recio, "Basilar-membrane response to multicomponent stimuli in chinchilla," *J. Acoust. Soc. Am.* vol. 110, pp. 981–994, 2001.